© 2018. Published by The Company of Biologists Ltd | Journal of Cell Science (2018) 131, jcs213009. doi:10.1242/jcs.213009

RESEARCH ARTICLE

GRWD1 regulates ribosomal protein L23 levels via the ubiquitin-proteasome system

Shinya Watanabe[1], Hiroki Fujiyama[1], Takuya Takafuji[1], Kota Kayama[1], Masaki Matsumoto[2], Keiichi I. Nakayama[2], Kazumasa Yoshida[1], Nozomi Sugimoto[1,*] and Masatoshi Fujita[1,*]

ABSTRACT

Glutamate-rich WD40 repeat-containing 1 (GRWD1) is a Cdt1-binding protein that promotes mini-chromosome maintenance (MCM) loading through its histone chaperone activity. GRWD1 acts as a tumor-promoting factor by downregulating p53 (also known as TP53) via the RPL11–MDM2–p53 axis. Here, we identified GRWD1-interacting proteins using a proteomics approach and showed that GRWD1 interacts with various proteins involved in transcription, translation, DNA replication and repair, chromatin organization, and ubiquitin-mediated proteolysis. We focused on the ribosomal protein ribosomal protein L23 (RPL23), which positively regulates nucleolar stress responses through MDM2 binding and inhibition, thereby functioning as a tumor suppressor. Overexpression of GRWD1 decreased RPL23 protein levels and stability; this effect was restored upon treatment with the proteasome inhibitor MG132. EDD (also known as UBR5), an E3 ubiquitin ligase that interacts with GRWD1, also downregulated RPL23, and the decrease was further enhanced by co-expression of GRWD1. Conversely, siRNA-mediated GRWD1 knockdown upregulated RPL23. Co-expression of GRWD1 and EDD promoted RPL23 ubiquitylation. These data suggest that GRWD1 acts together with EDD to negatively regulate RPL23 via the ubiquitin-proteasome system. GRWD1 expression reversed the RPL23-mediated inhibition of anchorage-independent growth in cancer cells. Our data suggest that GRWD1-induced RPL23 proteolysis plays a role in downregulation of p53 and tumorigenesis.

KEY WORDS: GRWD1, RPL23, EDD, p53, Ubiquitin, Proteasome, Nucleolar stress

INTRODUCTION

Glutamate-rich WD40 repeat containing 1 (GRWD1) is a member of the WD protein family and is highly conserved in eukaryotes. The budding yeast GRWD1 homolog, Rrb1, is essential for cell growth and required for the early steps in ribosome assembly (Iouk et al., 2001; Schaper et al., 2001). In yeast, it interacts with Rpl3, a ribosomal protein, and functions as a chaperone for Rpl3 (Iouk et al., 2001; Pausch et al., 2015). In addition, GRWD1 in human cells may be involved in ribosome biogenesis (Gratenstein et al., 2005; Kayama et al., 2017), although detailed studies are lacking. For example, it is not clear whether GRWD1 interacts with some other ribosome proteins.

GRWD1 also belongs to the family of DNA damage-binding protein 1 (DDB1)-interacting WD40 proteins, which function as candidate substrate receptors for Cul4–DDB1 ubiquitin ligases (note that there are Cul4a and Cul4b forms of Cul4 in mammals) (He et al., 2006; Higa et al., 2006). For example, Cdt2, a Cul4–DDB1-interacting WD40 protein, is a receptor for Cdt1, a replication-licensing factor. However, a substrate(s) of the Cul4–DDB1–GRWD1 ubiquitin ligase remains to be identified.

In addition, Rrb1 interacts with the replication initiation protein origin recognition complex (ORC) subunit 6 (ORC6), and its inactivation delays the metaphase-to-anaphase transition (Killian et al., 2004). Rrb1 binds to yeast pescadillo homolog 1 (Yph1), which functions cooperatively with the ORC and mini-chromosome maintenance 2–7 (MCM2–7) DNA replication helicase proteins (Du and Stillman, 2002). In human cells, we identified GRWD1 as a novel Cdt1-binding protein (Sugimoto et al., 2008). CDC6 and Cdt1 bind to the ORC at replication origins from late M phase to G_1 phase and load MCM2–7 onto chromatin, resulting in formation of the pre-replication complex (pre-RC). In this context, GRWD1 functions as a histone chaperone to promote MCM loading at replication origins (Aizawa et al., 2016; Sugimoto et al., 2015).

Furthermore, recent evidence from our group demonstrates that GRWD1 negatively regulates p53 (also known as TP53), an important tumor suppressor (Kayama et al., 2017). GRWD1 is overexpressed in several cancer cell lines (Sugimoto et al., 2015). Consistent with these findings, overexpression of GRWD1 induces oncogenic transformation in normal human cells and is associated with poor prognosis in cancer patients (Kayama et al., 2017). Therefore, it is important to ascertain the effects of GRWD1 overexpression. The p53-suppressing activity of GRWD1 is likely to be executed (mainly) via its direct binding to and sequestering of ribosomal protein L (RPL)-11 from the mouse double minute (MDM)-2 ubiquitin ligase, which proteolytically inhibits p53 (Kayama et al., 2017). Ribosome proteins are important components of ribosomes. However, increasing attention is being paid to certain ribosomal proteins that act as tumor suppressors (Takafuji et al., 2017). RPL11 and RPL5, both of which are components of the large ribosomal subunit, are tumor-suppressive ribosomal proteins; these proteins work together and act as crucial regulators of p53-mediated responses to nucleolar stress by interacting with MDM2 and repressing its ubiquitin ligase activity. In addition, RPL5 and RPL11 play an important role in the induction of p53 by DNA double-strand breaks or hypergrowth stimuli, such as activated RAS or c-Myc overexpression (Bursac et al., 2012; Macias et al., 2010; Morgado-Palacin et al., 2015; Nishimura et al., 2015; Takafuji et al., 2017). Nevertheless, the molecular mechanisms by which overexpressed GRWD1 transforms cells are unclear.

[1]Department of Cellular Biochemistry, Graduate School of Pharmaceutical Sciences, Kyushu University, Fukuoka 812-8582, Japan. [2]Department of Molecular and Cellular Biology, Medical Institute of Bioregulation, Kyushu University, Fukuoka 812-8582, Japan.

*Authors for correspondence (sugimoto@phar.kyushu-u.ac.jp; mfujita@phar.kyushu-u.ac.jp)

N.S., 0000-0002-4313-5728; M.F., 0000-0001-6617-2452

Received 12 November 2017; Accepted 11 June 2018

Journal of Cell Science (2018) 131, jcs213009. doi:10.1242/jcs.213009

As described above, GRWD1 is a multi-functional protein involved in multiple cellular regulatory pathways associated with the control of cell growth. Therefore, a clear understanding of the function and regulation of GRWD1 is important. To address this, we comprehensively identified GRWD1-interacting proteins using immunoprecipitation combined with mass spectrometry (IP-MS). Our results demonstrated that GRWD1 interacts with various proteins involved in transcription, translation, cell cycle progression, DNA replication, repair, chromatin organization and ubiquitin-mediated proteolysis. Among the proteins identified, we focused on the ribosomal protein RPL23. RPL23 interacts directly with MDM2, and this interaction is enhanced in response to actinomycin D (Act D) treatment (Dai et al., 2004; Jin et al., 2004). Overexpression of RPL23 alleviates MDM2-mediated p53 ubiquitylation and stabilizes p53 levels (Dai et al., 2004; Jin et al., 2004). RPL5, RPL11 and RPL23 bind to MDM2 simultaneously, forming a heterotetramer within cells (Dai and Lu, 2004). Although knockdown of RPL5 or RPL11, but not RPL23, markedly inhibits Act D-driven p53 induction (Bursac et al., 2012; Nicolas et al., 2016), evidence suggests that RPL23 functions as a tumor suppressor (Meng et al., 2016; Zhang et al., 2010, 2013). The present data suggest that GRWD1 acts together with the E3 ubiquitin ligase EDD [also known as human (h)HYD or UBR5] and proteolytically regulates RPL23, and that this regulatory mechanism may play a role in p53 downregulation by GRWD1.

RESULTS

Comprehensive identification of GRWD1-interacting proteins

Anti-FLAG IP-MS was performed using cell extracts from 293T cells transfected with HA–GRWD1–FLAG or HA–GRWD1 as a control in a buffer containing 150 mM NaCl as reported previously (Kayama et al., 2017). Proteins containing four or more peptides with ion scores >45 in a MASCOT search and with a number of peptide fragments ≥4-fold higher than that of the control samples were selected. As a result, 182 proteins were identified as GRWD1 interactors (Fig. 1A; Table S1), among which RPL5, RPL11 and RPL23 had been reported previously (Kayama et al., 2017). IP was also performed using nuclear extracts prepared from 293T cells transfected with HA–GRWD1–FLAG or HA–GRWD1 as a control in a high-salt (500 mM NaCl) buffer to identify insoluble proteins, followed by MS analysis (Fig. 1B). Thereby, 109 proteins were identified (Fig. 1A; Table S2). A comparison of proteins detected under the two different conditions identified 72 that were common under both (Fig. 1A). Among the proteins identified by IP-MS, DDB1, NOC2L, Topo I, VCP and WDR5 have been previously reported as GRWD1-interacting proteins (https://www.ncbi.nlm.nih.gov/gene/83743; Fogeron et al., 2013; He et al., 2006; Higa et al., 2006; Trzcińska et al., 2002; Wan et al., 2015). The interaction between some of these proteins and GRWD1 was further assessed by IP and immunoblotting using 293T cells (Fig. 1C). The 219 GRWD1-interacting proteins identified were classified according to their functions based on PANTHER (http://pantherdb.org) and previous studies (Sugimoto et al., 2015). Approximately 30% were proteins involved in translation, including ribosomal proteins (RPs) and nucleolar proteins (Fig. 1D). This finding is consistent with a previous report suggesting that GRWD1 may be involved in ribosome biogenesis (Gratenstein et al., 2005). Moreover, GRWD1 interacts with various transcription-associated factors (~15%; Fig. 1D). This supports the notion previously suggested by our group that GRWD1 may function not only in DNA replication but also in transcription (Sugimoto et al., 2015). Data from the present MS analysis and the STRING database (http://string-db.org) predicted physical and functional interactions among proteins associated with translation (Fig. 1E) and cell cycle control, as well as DNA replication (Fig. S1A) and transcription (Fig. S1B). Taken together, these data indicate that GRWD1 functions in association with various proteins involved in a variety of cellular processes, especially those associated with the nucleus and nucleolus.

GRWD1 interacts with RPL23 and regulates its expression together with the EDD ubiquitin ligase

GRWD1 downregulates p53 (Kayama et al., 2017), and RPL23 is involved in the modulation of p53 levels (Dai and Lu, 2004; Dai et al., 2004; Jin et al., 2004); therefore, we focused on RPL23 based on the hypothesis that the GRWD1–RPL23 interaction could play a role in GRWD1-mediated p53 downregulation.

First, the interaction between GRWD1 and RPL23 was confirmed. 293T cells or HCT116 cells were subjected to IP with an anti-GRWD1 antibody. As shown in Fig. 2A, endogenous GRWD1 co-precipitated endogenous RPL23 in both cell lines. Reciprocal co-IP analysis also demonstrated that exogenous RPL23–FLAG co-precipitates endogenous GRWD1 (Fig. 2B). *In vitro* pulldown assays with purified proteins indicated that GRWD1 directly binds to RPL23 (Fig. 2C,D).

To investigate the physiological significance of the GRWD1–RPL23 interaction, HCT116 cells were transfected with a HA–GRWD1-expressing vector along with a construct expressing RPL5–FLAG, RPL11–FLAG or RPL23–FLAG. Western blot analysis showed that GRWD1 overexpression downregulated RPL23, whereas it had little effect on RPL5 and RPL11 (Fig. 3A). Similar results were obtained when non-tagged GRWD1 was overexpressed (Fig. S2A) and with 293T cells (Fig. S2B). RPL23 downregulation was partially suppressed by treatment with the proteasome inhibitor MG132 (Fig. 3B), suggesting that GRWD1 reduces RPL23 protein levels through the ubiquitin-proteasome pathway. We investigated the effect of GRWD1 overexpression on levels of endogenous RPL23 and some other ribosomal proteins. RPL23, but not RPL3, RPL5 and RPL11, levels fell upon overexpression of GRWD1 (Fig. 3C, whole-cell fraction). To identify whether the reduced expression of RPL23 seen upon overexpression of GRWD1 occurs in the soluble or nucleolar fraction, we performed a cell fractionation assay as described in the Materials and Methods. We found that the NP-40 supernatant fraction contained mainly free and ribosome-incorporated RPs, and that the final pellet fraction contained nucleoli (Bhat et al., 2004; Harlow and Lane, 1988). In both the NP-40 supernatant and pellet fraction, overexpression of GRWD1 downregulated RPL23 specifically (Fig. 3C). As expected, α-tubulin was detected mainly in the NP-40 supernatant fraction and fibrillarin was enriched in the pellet fraction (Fig. 3C). It is conceivable that GRWD1 overexpression could affect soluble RPL23 primarily, and that such a reduction could lead to reduced levels of ribosome-incorporated and nucleolus-incorporated RPL23 proteins. To examine whether GRWD1 overexpression affects the stability of RPL23, we added cycloheximide (CHX) to HA–GRWD1-overexpressing HFF2/T cells and monitored protein levels (Fig. 3D). The data revealed that GRWD1 overexpression destabilized endogenous RPL23 proteins.

Next, we searched for an E3 ubiquitin ligase involved in RPL23 ubiquitylation. EDD was among the E3 ubiquitin ligases identified by MS analysis of GRWD1-interacting proteins (Tables S1 and S2). EDD belongs to the HECT family of E3 ubiquitin ligases (Rotin and Kumar, 2009) and regulates the stability of various proteins such as topoisomerase II β-binding protein 1 (TopBP1) and Tat-interactive

Journal of Cell Science (2018) 131, jcs213009. doi:10.1242/jcs.213009

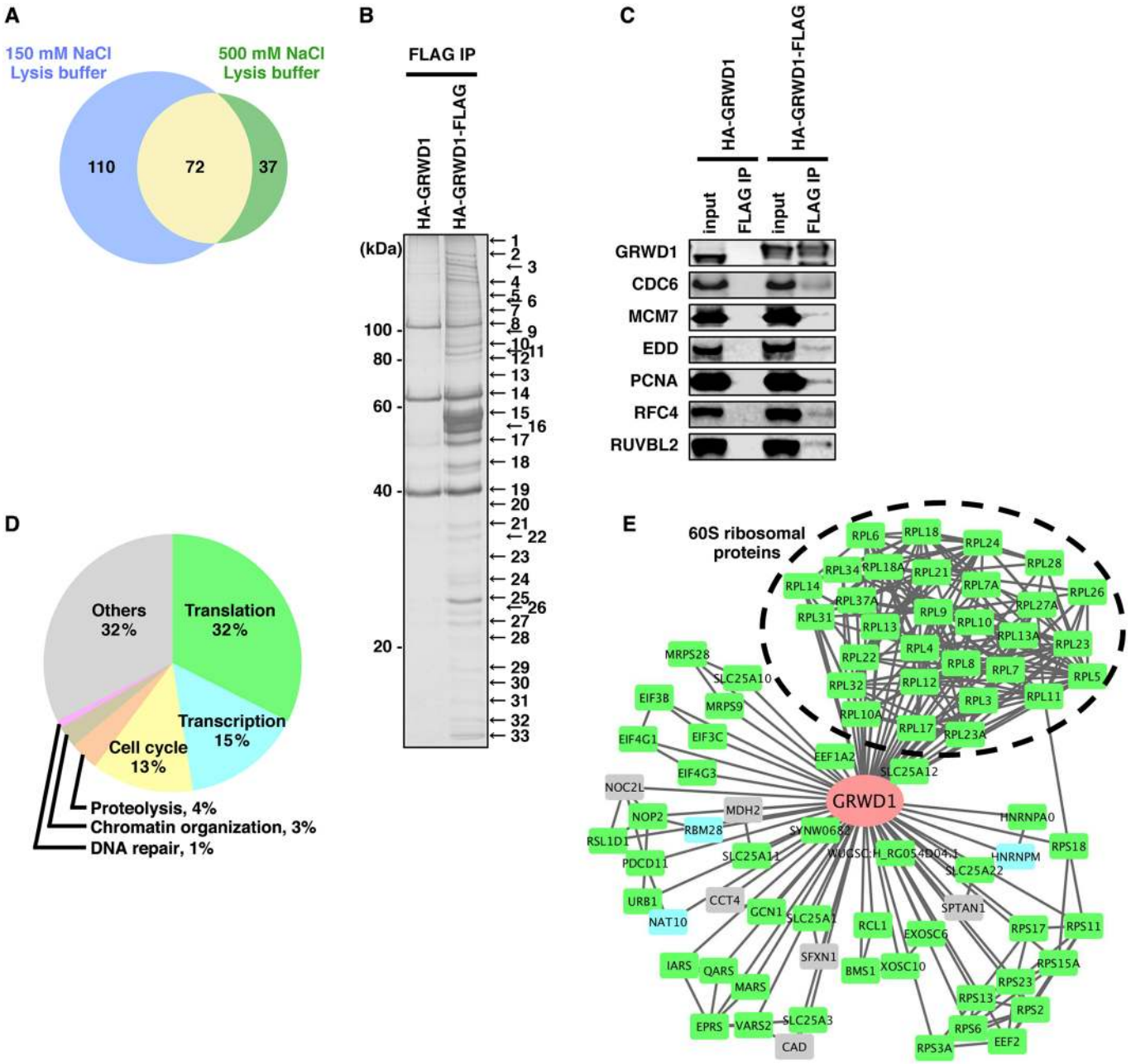

Fig. 1. Identification of GRWD1-interacting proteins and their potential physical and functional networks. (A) Venn diagram representing GRWD1-interacting proteins obtained with lysis buffer containing 150 mM NaCl or 500 mM NaCl. (B) 293T cells were transiently transfected with HA–GRWD1–FLAG or HA–GRWD1 as a control and extracted with high-salt (500 mM NaCl) buffer. Lysates were immunoprecipitated with anti-FLAG antibody, and immunoprecipitated proteins (IP) were analyzed by SDS-PAGE and silver staining. The gel was cut into 33 slices according to the visible bands and numbered as shown on the right. Proteins in each gel slice were digested with trypsin, and peptides were detected by liquid chromatography-MS/MS analysis. (C) 293T cells were transiently transfected with HA–GRWD1 or HA–GRWD1–FLAG expression vectors and lysed in high-salt buffer. Lysates were immunoprecipitated with anti-FLAG antibody, and immunoprecipitated proteins and 2.6% of the input were analyzed by immunoblotting with the indicated antibodies. (D) Functional classification of 219 GRWD1-interacting proteins. GRWD1-interacting proteins were classified according to function based on PANTHER (http://pantherdb.org) and the literature. (E) Physical and functional interactions among GRWD1-interacting proteins associated with translation. The map was generated using information obtained from the present MS analysis and the STRING database (http://string-db.org). The color of each protein coincides with that in Fig. 1D.

protein 60 (TIP60) (Honda et al., 2002; Subbaiah et al., 2016). The interaction between EDD and GRWD1 was confirmed by co-IP and immunoblotting (Fig. 1C). Overexpression of EDD decreased RPL23 protein levels in HCT116 cells; however, this reduction was less pronounced after treatment with MG132 (Fig. 3E). Moreover, RPL23 degradation induced by EDD overexpression was increased by co-expression of GRWD1 (Fig. 3E).

To further examine whether GRWD1 and EDD contribute to regulation of endogenous RPL23 protein levels, GRWD1 was knocked down using siRNAs and RPL23 levels were quantified. Depletion of GRWD1 increased RPL23 protein levels in HeLa (Fig. 4A, left panel) and HCT116 (Fig. 4B, 0 h) cells. Given that GRWD1 interacts with various transcription factors (Fig. 1), we examined whether GRWD1 affects RPL23 mRNA transcription.

Journal of Cell Science (2018) 131, jcs213009. doi:10.1242/jcs.213009

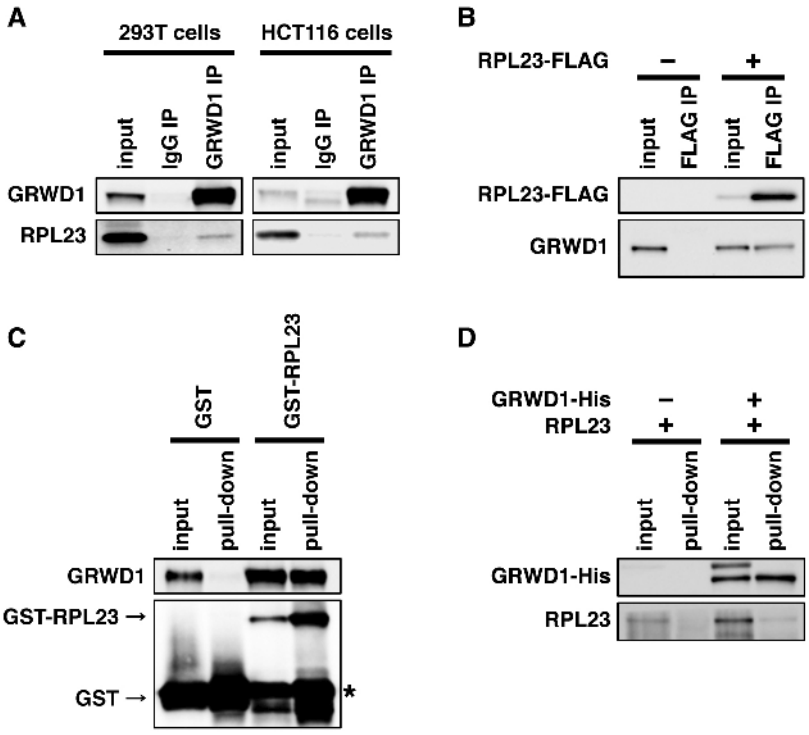

Fig. 2. GRWD1 interacts with RPL23. (A) 293T or HCT116 cells were subjected to immunoprecipitation (IP) with anti-GRWD1 antibody or control IgG. The immunoprecipitated proteins and 2.2% of the input were analyzed by SDS-PAGE and immunoblotting with the indicated antibodies. (B) HCT116 cells were transiently transfected for 42 h with the indicated expression vectors (12 µg) and then subjected to immunoprecipitation with anti-FLAG antibody. The immunoprecipitated proteins and 1% of the input were immunoblotted with the indicated antibodies. (C) GST–RPL23 or GST alone was incubated with purified GRWD1, and bound proteins and 15% of the input were analyzed by SDS-PAGE and immunoblotting with the indicated antibodies. The asterisk indicates degradation and/or immature products of GST–RPL23. (D) GRWD1–His or buffer alone was incubated with purified RPL23; bound proteins and 15% of the input were then immunoblotted with the indicated antibodies.

GRWD1 silencing had no effect on RPL23 mRNA levels in HCT116 and HeLa cells (Fig. 4A, right panel). GRWD1 silencing upregulated RPL23 even in the presence of low doses of Act D, an inducer of nucleolar stress (Iapalucci-Espinoza and Franze-Fernández, 1979; Perry and Kelley, 1970) (Fig. 4B). Similar results were obtained using different siRNAs targeting GRWD1 (Fig. S3). GRWD1 is functionally implicated in ribosome biogenesis (Gratenstein et al., 2005; Iouk et al., 2001; Schaper et al., 2001), and silencing of GRWD1 actually impairs nucleolar integrity and thereby induces the nucleolar stress response (Kayama et al., 2017); therefore, if we used only data obtained from endogenous GRWD1-depleted cells, it would be difficult to clarify whether GRWD1 directly regulates RPL23 via the ubiquitin-proteasome system directly or whether nucleolar stress responses affect RPL23 levels. However, the data showing that silencing GRWD1 increases RPL23 protein levels are in line with the model that GRWD1 regulates RPL23 directly via the ubiquitin-proteasome system.

Depletion of EDD also moderately increased RPL23 in HCT116 cells treated with or without Act D (Fig. 4C). GRWD1 depletion stabilized p53 levels (Fig. 4B) as reported previously (Kayama et al., 2017), and EDD depletion also increased p53 levels (Fig. 4C), suggesting that the modulation of RPL23 by GRWD1 and EDD contributes to p53 regulation. Taken together, these data suggest that GRWD1 and EDD cooperatively regulate RPL23 protein levels via the ubiquitin-proteasome pathway.

As GRWD1 interacts with various E3 ubiquitin ligases (Tables S1 and S2), it is possible that other ubiquitin ligase(s) that form a complex with GRWD1 also destabilize RPL23. Given that GRWD1 interacts with the Cul4–DDB1 ubiquitin ligase complex (He et al., 2006; Higa et al., 2006), and the present MS analysis identified DDB1 as a GRWD1-interacting protein (Table S1), we examined whether overexpression of Cul4a and/or DDB1 affects RPL23. Overexpression of Cul4a did not affect RPL23 protein levels, whereas overexpression of DDB1 downregulated RPL23 in 293T cells (Fig. S4A). EDD and DDB1 form a complex that functions as an ubiquitin ligase (Jung et al., 2013; Maddika and Chen, 2009; Wang et al., 2013). We therefore tested the interactions between GRWD1, EDD and DDB1. Overexpression of FLAG–DDB1 inhibited the co-immunoprecipitation of FLAG–EDD with HA–GRWD1 in 293T cells (Fig. S4B), suggesting that GRWD1 forms a distinct complex with EDD or DDB1. However, the mechanism underlying the effect of DDB1 on RPL23 protein levels remains unclear.

GRWD1 interacts with RPL23 via its N-terminal domain

To determine the region(s) of GRWD1 necessary for the RPL23 interaction, we performed a pulldown assay using GST–RPL23 and lysates from 293T cells transiently expressing truncated GRWD1 mutants (Fig. 5A,B). Full-length (FL) GRWD1 or the GRWD1 Nter-WD40 mutant interacted with GST–RPL23, whereas the interaction of GRWD1 Δacid with GST–RPL23 was reduced (Fig. 5B). No interaction was observed with GRWD1 Mid-Cter. Co-IP assays confirmed the reduced interaction of GRWD1 Δacid or Mid-Cter with RPL23 (Fig. 5C). These results indicate that GRWD1 interacts with RPL23 via the N-terminal domain, including the acidic domain. Next, we investigated the effects of the mutations on the ability of GRWD1 to downregulate RPL23. Overexpression of GRWD1 Mid-Cter, which does not bind RPL23, downregulated RPL23 to a lesser extent (Fig. 5D). GRWD1 Δacid overexpression reduced RPL23 levels despite the weak interaction between GRWD1 Δacid and RPL23, suggesting that GRWD1 Δacid retains a partial ability to interact with RPL23 (Fig. 5D). The reason why GRWD1 Nter-WD40, which binds to RPL23, showed an impaired ability to reduce RPL23 levels remains unclear.

GRWD1 and EDD promoted the ubiquitylation of RPL23

To obtain further evidence that GRWD1 and EDD regulate RPL23 protein levels via the ubiquitin-proteasome system, *in vivo* ubiquitylation assays were performed using 293T cells

Journal of Cell Science (2018) 131, jcs213009. doi:10.1242/jcs.213009

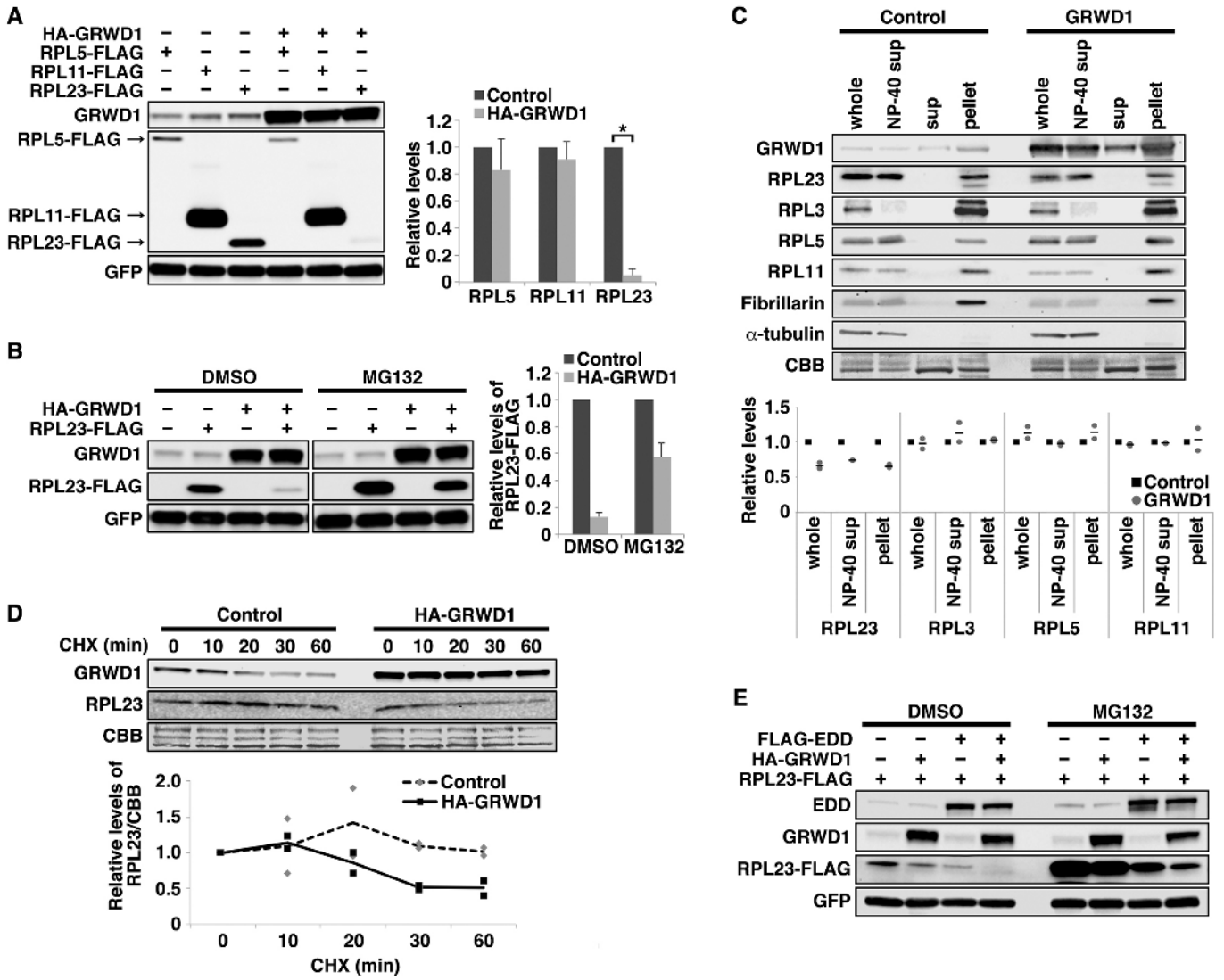

Fig. 3. GRWD1 and EDD cooperatively promote proteasome-dependent RPL23 proteolysis. (A) HCT116 cells were transiently transfected for 42 h with the indicated expression vectors (RPLs–FLAG, 0.48 µg; HA–GRWD1, 0.32 µg; or GFP, 0.04 µg) and analyzed by SDS-PAGE and immunoblotting with the indicated antibodies. GFP served as a control protein to show equal transfection efficiencies. The signal intensities of the bands were quantified as described in the Materials and Methods. The signals were further normalized to the signal generated by control GFP. The mean±s.d. from four independent experiments is shown in the right panels. Values for control samples lacking HA–GRWD1 overexpression are set at 1. *P<0.05 (two-tailed Student's t-test). (B) HCT116 cells were transiently transfected with the indicated expression vectors (RPLs–FLAG, 0.48 µg; HA–GRWD1, 0.32 µg; or GFP, 0.04 µg) for 30 h, treated with or without the proteasome inhibitor MG132 (25 µM) for a further 12 h, and then analyzed by SDS-PAGE and immunoblotting with the indicated antibodies. The signal intensity of RPL23–FLAG was measured and further normalized to the signal generated by GFP. The mean±s.d. from three independent experiments is shown in the right panels, with values for control samples lacking HA–GRWD1 overexpression set as 1. (C) HCT116 cells were transiently transfected for 42 h with the indicated expression vectors (12 µg) and subjected to cell fractionation as described in the Materials and Methods. Each fraction was isolated and analyzed with the indicated antibodies. The signal intensities of the bands were quantified, and the mean and individual data points from two independent experiments are shown in the lower panel (values for the control sample are set as 1). (D) Half-life of RPL23. Control and HA–GRWD1-overexpressing HFF2/T cells were treated with 50 µg/ml cycloheximide and harvested at the indicated times. Whole-cell extracts (whole) were analyzed by immunoblotting with the indicated antibodies. The signal intensities of the bands were quantified, and the means and individual data points from two independent experiments are shown. CBB staining was used as a loading control. (E) HCT116 cells were transiently transfected with the indicated expression vectors (RPL23–FLAG, 0.4 µg; HA–GRWD1, 0.1 µg; FLAG–EDD, 0.3 µg; or GFP, 0.04 µg) for 36 h, treated with or without MG132 (25 µM) for a further 12 h, and then analyzed by SDS-PAGE and immunoblotting with the indicated antibodies.

transfected with RPL23–FLAG, HA-tagged ubiquitin (HA-Ub), FLAG–EDD and HA–GRWD1 expression vectors in various combinations. After 36 h, the cells were treated with MG132 for 12 h to prevent the degradation of RPL23. The cellular extracts were then immunoprecipitated with anti-RPL23 antibody, and the immunoprecipitates were analyzed by immunoblotting. Overexpression of GRWD1 or EDD promoted RPL23 ubiquitylation, as indicated by a smear of high molecular mass RPL23 bands, and this effect was further enhanced by co-transfection of GRWD1 and EDD (Fig. 6). These results supported the notion that GRWD1 and EDD cooperatively ubiquitylate and downregulate RPL23.

GRWD1 modulates MDM2 protein levels by regulating RPL23

Finally, the biological relevance of GRWD1-mediated regulation of RPL23 was investigated. MDM2 ubiquitylates and degrades not

Journal of Cell Science (2018) 131, jcs213009. doi:10.1242/jcs.213009

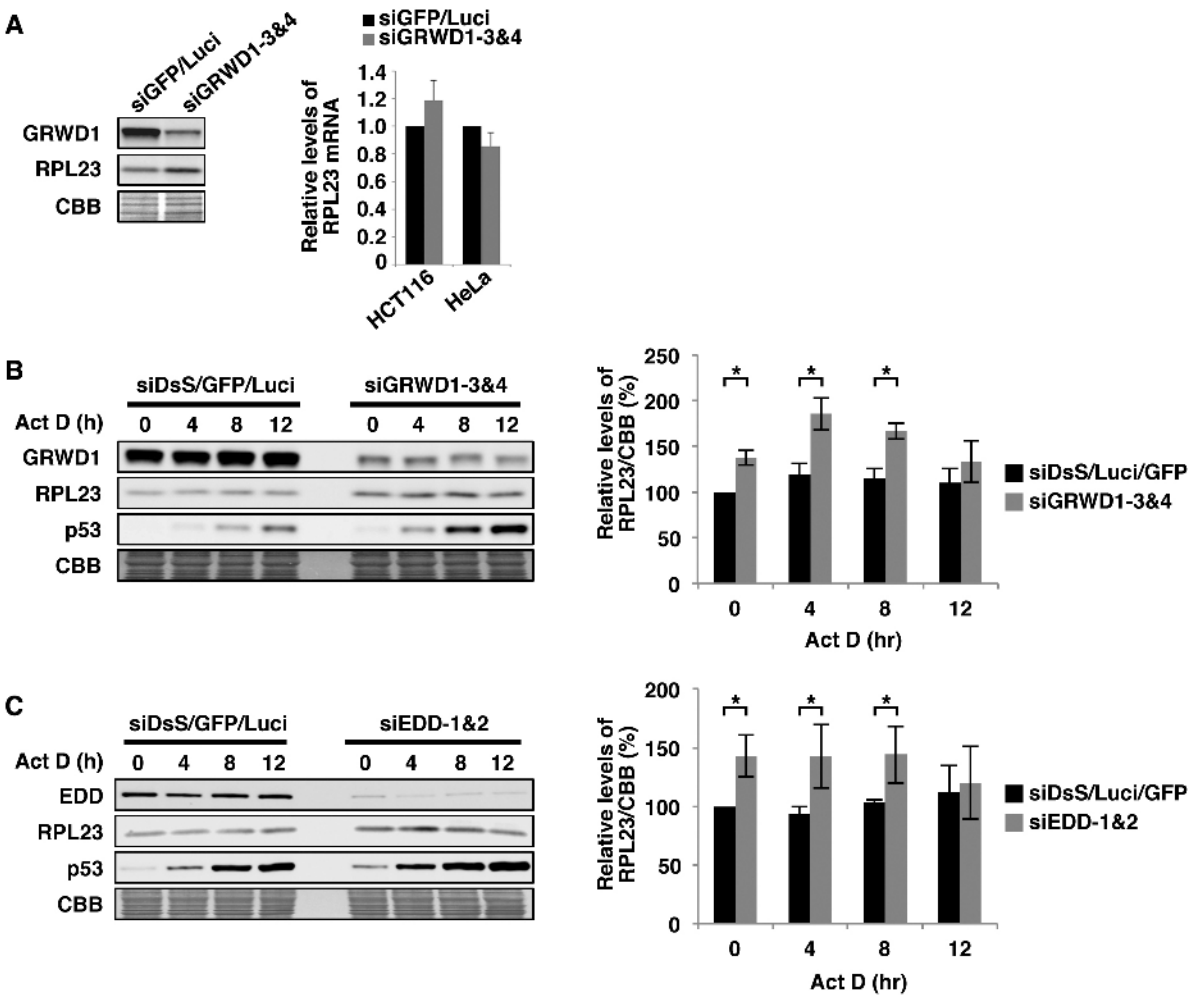

Fig. 4. siRNA-mediated GRWD1 or EDD knockdown increases RPL23 protein levels in cells treated with a low dose of actinomycin D. (A) Left panel: HeLa cells were transfected with control (a mixture of siGFP and siLuci; siGFP/Luci) or GRWD1-targeting (a mixture of siGRWD1-3 and -4; siGRWD1-3&4) siRNAs for 48 h. Whole-cell extracts were analyzed by SDS-PAGE and immunoblotted with the indicated antibodies. CBB staining was used as a loading control. Right panel: HeLa and HCT116 cells were transfected with control or GRWD1-targeting siRNAs as above. Total RNAs were prepared, and the relative levels of RPL23 mRNA to control GAPDH mRNA were determined by reverse transcriptase quantitative PCR. The mean±s.d. from three independent experiments is shown with the values of control siGFP/Luci-treated samples set as 1. (B,C) HCT116 cells were transfected with control (mixture of control DS scrambled Neg, siLuci, and siGFP; siDsS/GFP/Luci) or GRWD1-targeting (siGRWD1-3&4) siRNAs (B), or EDD-targeting (mixture of siEDD-1 and -2; siEDD-1&2) siRNAs (C) for 24 h, followed by actinomycin D (5 nM) and harvesting at the indicated times. Whole-cell extracts were analyzed by SDS-PAGE and immunoblotting with the indicated antibodies. CBB staining was used as a loading control. The signal intensities of the bands were quantified, and the mean±s.d. from three (B) or five (C) independent experiments are shown in the right panels with the 0 h control sample values set at 100%. **P*<0.05 (two-tailed Student's *t*-test).

only p53 but also MDM2 itself. In addition, RPL23 inhibits MDM2 ubiquitin ligase activity. Therefore, RPL23 may act as a tumor suppressor (Dai et al., 2004; Jin et al., 2004; Meng et al., 2016; Zhang et al., 2010, 2013). By contrast, our previous study identified GRWD1 as a novel negative regulator of p53 and a potential oncogene (Kayama et al., 2017). Therefore, we hypothesized that GRWD1-mediated RPL23 downregulation leads to MDM2 activation and thus contributes to tumorigenesis. To test this, we used colon cancer-derived HCT116 cells. The results showed that overexpression of RPL23 increased MDM2 protein levels in HCT116 cells (Fig. 7A). However, co-overexpression of GRWD1 reduced RPL23 protein levels and repressed MDM2 upregulation (Fig. 7A). These data indicate that GRWD1 affects MDM2 ubiquitin ligase activity by modulating RPL23.

Next, we investigated the effects of GRWD1 and RPL23 expression on tumor cell proliferation. HCT116 cells stably overexpressing GRWD1 were first established, as detailed in the Materials and Methods. Then, parental and GRWD1-overexpressing HCT116 cells were infected with high-titer retrovirus to introduce RPL23 and subjected to soft agar colony formation assays. Expression of exogenous GRWD1 and T7-RPL23 and suppression of T7-RPL23 by GRWD1 overexpression were confirmed by immunoblotting (Fig. 7B). Parental cells overexpressing RPL23 formed significantly fewer colonies than those harboring the control vector (Fig. 7C). This finding was consistent with previous reports (Meng et al., 2016; Zhang et al., 2010, 2013). Interestingly, RPL23-mediated growth suppression was restored by co-expression of GRWD1 (Fig. 7C). These results suggest that GRWD1 promotes anchorage-independent tumorigenic cell growth by downregulating RPL23.

DISCUSSION

A comprehensive search for novel GRWD1-interacting proteins identified various proteins mainly involved in transcription,

Journal of Cell Science (2018) 131, jcs213009. doi:10.1242/jcs.213009

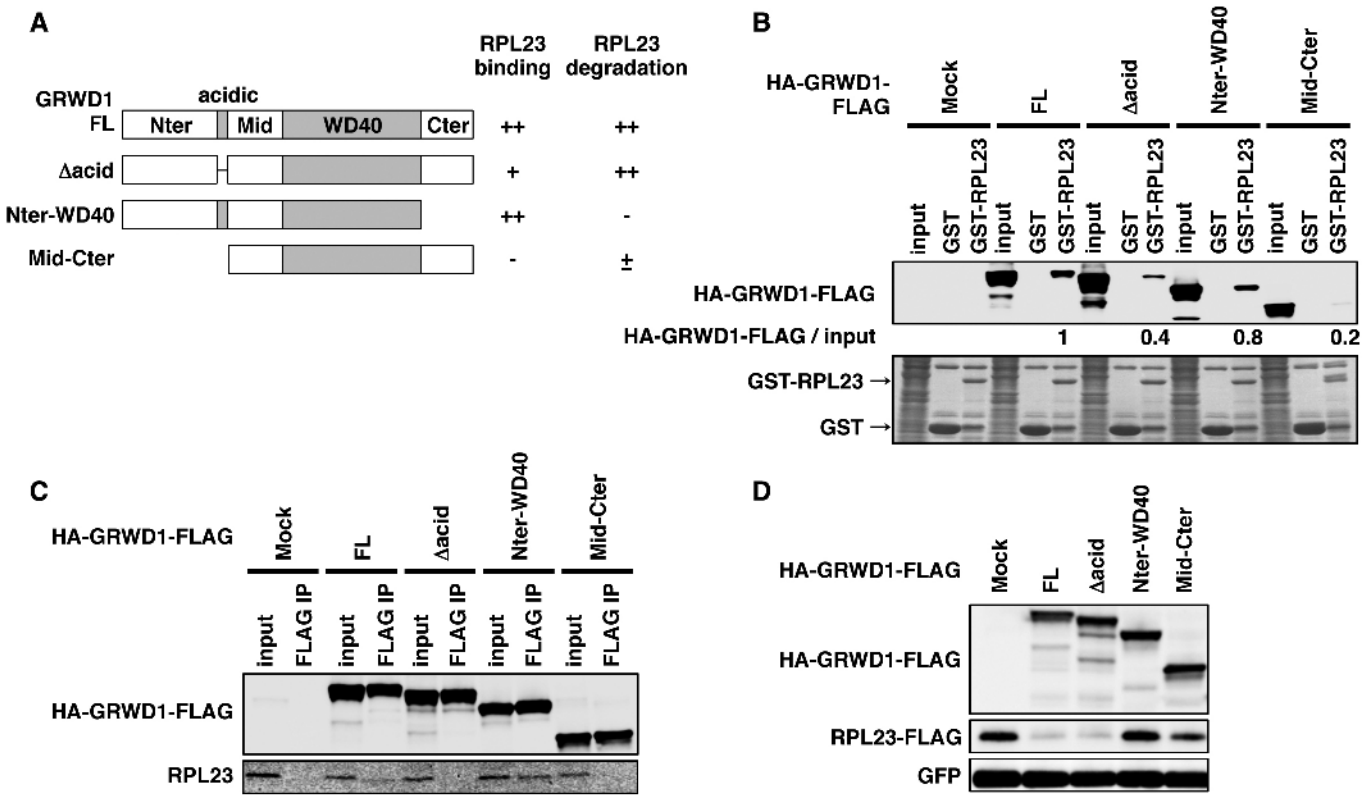

Fig. 5. GRWD1 interacts with RPL23 via its N-terminal domain. (A) Schematic representation of full-length (FL) GRWD1 and the truncated mutants used in the following studies. (B) 293T cells were transiently transfected with the indicated expression vectors (12 µg) for 42 h and lysed in NP-40 buffer. GST–RPL23 or GST alone was incubated with these lysates. Bound proteins and 6.3% of the input were analyzed by SDS-PAGE followed by immunoblotting with anti-FLAG antibody or CBB staining for detection of GST proteins. The signal intensities of HA–GRWD1–FLAG were quantified. To calculate co-precipitation efficiency, specific signals generated by precipitated proteins were normalized to signals generated by input proteins. Relative values are shown. The value for FL GRWD1 is set as 1. (C) 293T cells were transiently transfected with the indicated expression vectors (12 µg) for 48 h and then subjected to immunoprecipitation with anti-FLAG antibody. The immunoprecipitated proteins and 1.4% of the input were analyzed by SDS-PAGE and immunoblotting with the indicated antibodies. (D) 293T cells were transiently transfected with the indicated expression vectors (RPL23–FLAG, 0.5 µg; GRWD1–FLAG, 0.3 µg; or GFP, 0.04 µg) for 48 h and then analyzed by SDS-PAGE and immunoblotting with the indicated antibodies. GFP served as a control protein to show equal transfection efficiencies.

translation and cell cycle progression (Fig. 1). Furthermore, we demonstrated that GRWD1 regulates RPL23 protein levels via the ubiquitin-proteasome system (Figs 2, 3, 4 and 6), and showed that EDD, an E3 ubiquitin ligase that was identified as a GRWD1-interacting protein, is involved in RPL23 degradation (Figs 3, 4 and 6). We showed that GRWD1 and EDD cooperatively promote the ubiquitylation of RPL23 (Fig. 6), which led us to hypothesize that GRWD1 acts as a substrate recognition subunit of the EDD ubiquitin ligase complex. Consistent with our hypothesis, a GRWD1 truncated mutant unable to interact with RPL23 did not decrease RPL23 protein levels (Fig. 5). Further experiments suggested that the promotion of RPL23 proteolysis may play a role in GRWD1-mediated p53 downregulation and tumorigenesis (Fig. 7).

The present MS analysis suggests a novel function of GRWD1 in cell cycle control, including DNA replication, transcription and translation (Fig. 1; Fig. S1). For example, GRWD1 interacts with replication factor C (RFC) subunits that are required for PCNA loading (Ellison and Stillman, 2001; O'Donnell et al., 2001; Tsurimoto and Stillman, 1989, 1990); therefore, GRWD1 might act as a histone chaperone not only during replication licensing but also during DNA replication fork progression or DNA repair. This possibility should be addressed in future studies.

EDD and GRWD1 cooperatively promote RPL23 ubiquitylation and degradation (Figs 3, 4 and 6). However, our results also suggested that DDB1 is involved in downregulating RPL23 (Fig. S4A). As Cul4a overexpression does not decrease RPL23 protein levels, the Cul4a–DDB1–GRWD1 ubiquitin ligase complex is not likely to be involved in the regulatory mechanism identified in this study. Because EDD and DDB1 form an ubiquitin ligase complex (Jung et al., 2013; Maddika and Chen, 2009; Wang et al., 2013), we hypothesized that the EDD–DDB1–GRWD1 ubiquitin ligase complex might regulate RPL23 protein levels. However, our data indicate that GRWD1 might form mutually exclusive complexes with EDD and DDB1 (Fig. S4B). Further investigation is needed to clarify the mechanism of DDB1-mediated RPL23 downregulation.

The p53 tumor suppressor responds to various cellular stresses including ribosomal stress and oncogenic hypergrowth stimuli, and RPL11 and RPL5 act cooperatively to induce p53 in response to stress (Bursac et al., 2012; Macias et al., 2010; Morgado-Palacin et al., 2015; Nishimura et al., 2015; Takafuji et al., 2017). Recently, we showed that GRWD1 acts as a tumor-promoting factor by downregulating p53, and GRWD1-mediated p53 inhibition may occur via GRWD1 binding to, and sequestering of, RPL11 from MDM2 (Kayama et al., 2017). The present data indicate that the proteolysis-mediated regulation of RPL23 levels by GRWD1 and EDD may also be involved in the downregulation of p53 by GRWD1 (Fig. 7D). EDD is overexpressed in cancer cells (Clancy et al., 2003; Fuja et al., 2004) similar to GRWD1

Journal of Cell Science (2018) 131, jcs213009. doi:10.1242/jcs.213009

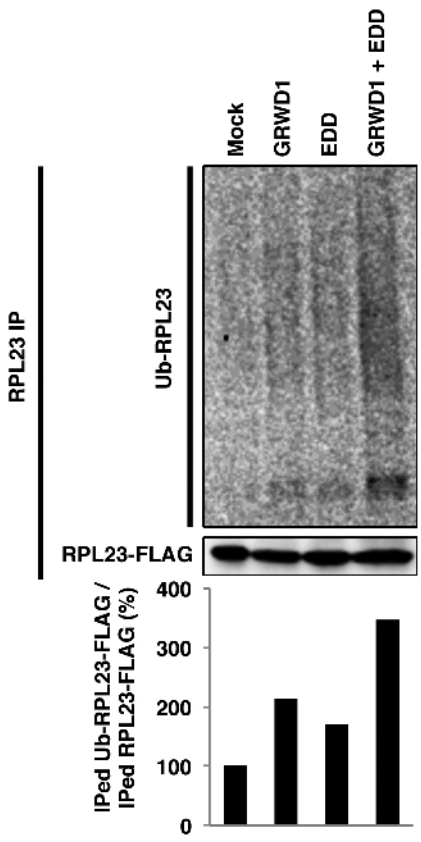

Fig. 6. GRWD1 and EDD cooperatively promote RPL23 ubiquitylation. 293T cells were transiently transfected with the indicated expression vectors (HA–Ub, 0.5 µg; RPL23–FLAG, 2.1 µg; HA–GRWD1, 0.16 µg; or EDD, 0.24 µg) for 36 h, and further treated with proteasome inhibitors for 12 h before harvest, followed by immunoprecipitation with anti-RPL23 antibody. The immunoprecipitated proteins were analyzed by immunoblotting with anti-HA (upper panel) or anti-FLAG (middle panel) antibodies. The signal intensities of the high molecular mass smears were quantified and are shown in the lower panel with the value of mock-transfected control sample set at 100. Experiment shown is representative of two repeats.

(Sugimoto et al., 2015), and its overexpression might also contribute to the suppression of p53 and increased tumorigenic potential.

We cannot rule out the possibility that GRWD1 affects p53 function and tumorigenesis through other mechanism(s). GRWD1 is a histone-binding protein that regulates chromatin throughout the genome (Aizawa et al., 2016; Sugimoto et al., 2015) and may also participate in the transcriptional control of rDNA (Iouk et al., 2001). In addition, GRWD1 interacts with various transcription-related factors (Fig. 1). Thus, it is possible that GRWD1 regulates the transcriptional activity of p53 by binding to p53-responsive promoters. On the other hand, expression of a dominant-negative mutant of BOP1, which is involved in rRNA processing, inhibits ribosomal biogenesis and elicits p53 activation (Pestov et al., 2001). Nuclear fractionation studies show that GRWD1 co-sediments with pre-ribosomal complexes and BOP1 (Gratenstein et al., 2005). Therefore, a complex including GRWD1 and BOP1 could also contribute to p53 regulation. Future studies should investigate the relationship between GRWD1 and p53 in detail.

GRWD1 interacts with various RPs, as well as with RPL11 and RPL23 (Fig. 1). While GRWD1 binds directly to RPL11 (Kayama et al., 2017) and RPL23 (Fig. 2), it is not clear whether it binds directly to the other RPs. Here, we identified RPL3 as a GRWD1-interacting protein (Fig. 1E; Table S2). In budding yeast, Rpl23 and Rpl3 bind in close proximity within the mature 60S subunit and share assembly interdependency (Gamalinda et al., 2014). In addition, Rrb1, a budding yeast homolog of GRWD1, interacts with Rpl3 and acts as a chaperone for Rpl3 (Iouk et al., 2001; Pausch et al., 2015). However, our results showed that GRWD1 may not regulate RPL3 protein levels (Fig. 3C). It will be important to investigate the relationship between GRWD1 and RPL3 in detail. In addition, we found that GRWD1 associates with RPS17 (Fig. 1E; Tables S1 and S2). Mutations of RPS17 are present in patients with Diamond–Blackfan anemia (Cmejla et al., 2007). Moreover, we identified RPL22 as a GRWD1-associating protein (Fig. 1E; Table S1). Somatic mutations in RPL22 are associated with T-cell acute lymphoblastic leukemia (Rao et al., 2012). Therefore, clarifying the relationship between RPs (i.e. RPS17 and RPL22) and GRWD1 would be important to further elucidate the oncogenic role of GRWD1.

MATERIALS AND METHODS

Cells

HCT116 cells were obtained from Bert Vogelstain (Johns Hopkins Kimmel Cancer Center, Baltimore, Maryland, USA). HeLa and HEK 293T cells (herein denoted 293T cells) were obtained from Masao Seto (Aichi Cancer Center Research Institute, Nagoya, Aichi, Japan). HFF2/T [non-transformed human fibroblasts immortalized with human telomere reverse transcriptase (hTERT)] cells were established in-house (Haga et al., 2007; Tatsumi et al., 2006). These cells were cryopreserved in small aliquots and passaged (for less than 6 months after resuscitation) in Dulbecco's modified Eagle's medium supplemented with 8% fetal calf serum. The cell lines have not been authenticated in-house. Tests for mycoplasma were performed as necessary.

Cycloheximide treatment

Cells were treated with 50 µg/ml cycloheximide (CHX) (Wako, Tokyo, Japan) and harvested at the indicated time points.

Immunoprecipitation

For Fig. 1B,C, 293T cells transiently transfected with the indicated expression vectors were lysed on ice in 400 µl high salt NP-40 buffer (500 mM NaCl, 1% NP-40 and 50 mM Tris-HCl pH 7.4) containing 1 mM DTT and multiple protease inhibitors. The soluble fractions were separated by centrifugation (13,600 ***g*** for 15 min) and diluted with 800 µl NP-40 buffer (150 mM NaCl, 1% NP-40, and 50 mM Tris-HCl pH 7.4). Lysates were immunoprecipitated with FLAG M2 Affinity Gel (Sigma, St Louis, MO), and the beads were washed three times with 1 ml NET gel buffer (150 mM NaCl, 0.1% Triton X-100 and 50 mM Tris-HCl pH 7.4). The immunoprecipitates were eluted with 3× FLAG Peptide (150 µg/ml, Sigma).

For Fig. 2A, 293T or HCT116 cells were lysed on ice in 1 ml NP-40 buffer containing 1 mM DTT and multiple protease inhibitors. The soluble fractions were separated by centrifugation (13,600 ***g*** for 15 min). Lysates were immunoprecipitated with anti-GRWD1 antibody (2 µg) and protein G–Sepharose, and the beads were washed three times with 1 ml NET gel buffer. The immunoprecipitates were eluted with 1× SDS sample buffer (62.5 mM Tris-HCl pH 6.8, 2% SDS, 5% β-mercaptoethanol, 10% glycerol and 0.01% Bromophenol Blue).

For Figs 2B and 5C, HCT116 or 293T cells transiently transfected with the indicated expression vectors were lysed on ice in 1 ml NP-40 buffer containing 1 mM DTT and multiple protease inhibitors. The soluble fractions were separated by centrifugation (13,600 ***g*** for 15 min). Lysates were immunoprecipitated with anti-FLAG antibody (4 µg) and protein G–Sepharose, and the beads were washed four times with 1 ml NET gel buffer. The immunoprecipitates were eluted with 1× SDS sample buffer.

For Fig. S4B, 293T cells transiently transfected with the indicated expression vectors were lysed on ice in 400 µl high-salt NP-40 buffer containing 1 mM DTT and multiple protease inhibitors. The soluble fractions were separated by centrifugation (13,600 ***g*** for 15 min) and diluted with 800 µl NP-40 buffer. Lysates were immunoprecipitated with

Journal of Cell Science (2018) 131, jcs213009. doi:10.1242/jcs.213009

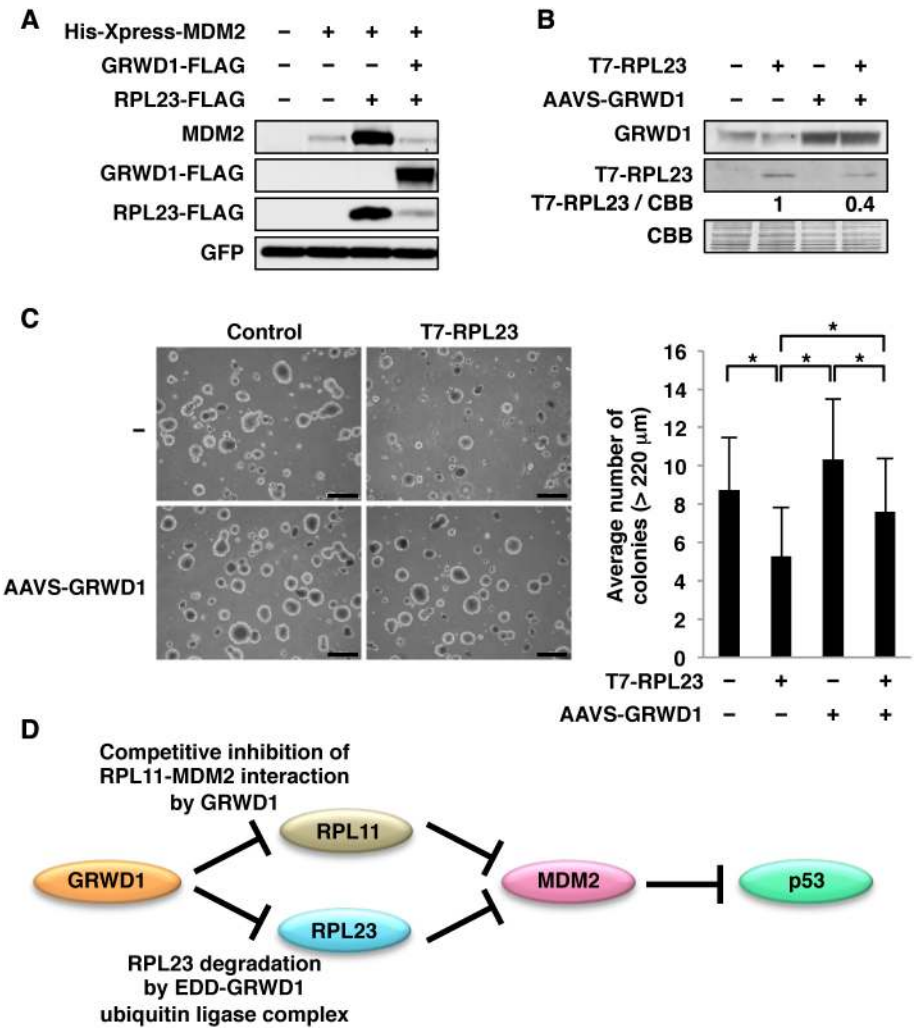

Fig. 7. GRWD1 regulates MDM2 protein levels by modulating RPL23. (A) HCT116 cells were transiently transfected with the indicated expression vectors (RPL23–FLAG, 0.4 µg; HA–GRWD1–FLAG, 0.2 µg; His-Xpress–MDM2, 0.2 µg; or GFP, 0.04 µg) for 48 h and then analyzed by SDS-PAGE and immunoblotting with the indicated antibodies. GFP served as a control protein to show equal transfection efficiencies. (B) Parental HCT116 cells or HCT116 AAVS-GRWD1 cells stably overexpressing GRWD1 were infected with a retrovirus vector expressing RPL23, selected with hygromycin B, and then analyzed by SDS-PAGE and immunoblotting with the indicated antibodies. The T7–RPL23 signal intensity was quantified and normalized to the signal generated by CBB bands. The obtained values are shown below. The control sample lacking GRWD1 overexpression is set as 1. (C) Anchorage-independent growth of HCT116 cells overexpressing RPL23 and/or GRWD1. At 18 days after seeding, images were acquired and colonies >220 µm in diameter were counted. Representative images are shown on the left. Scale bars: 500 µm. Average numbers of colonies per field, with s.d., are shown in the right panel; 12 randomly selected areas were counted per sample. *P<0.05 (Tukey's multiple comparison test performed after examination by one-way ANOVA). (D) Proposed model. In addition to GRWD1 inhibiting the RPL11–MDM2 interaction (Kayama et al., 2017), GRWD1 and EDD might form a complex and regulate RPL23 protein levels via the ubiquitin-proteasome system to downregulate p53.

anti-GRWD1 antibody (2 µg) and protein G-Sepharose, and the beads were washed four times with 1 ml NET gel buffer. The immunoprecipitates were eluted with 1× SDS sample buffer.

Mass spectrometry

The anti-FLAG immunoprecipitates were concentrated by trichloroacetic acid precipitation and then subjected to mass spectrometry as described previously (Kayama et al., 2017).

Cell lysate fractionation

Fractions were isolated from control or GRWD1-transfected HCT116 cells essentially as described previously, with slight modifications (Bhat et al., 2004). Briefly, cells grown in a 100 mm dish were trypsinized, pelleted, washed with PBS, and centrifuged at 100 ***g*** for 5 min. The cell pellet was then resuspended in 1 ml of RSB buffer (10 mM Tris-HCl pH 7.4, 10 mM NaCl, and 1.5 mM $MgCl_2$) and placed on ice for 10 min. Swollen cells were then collected by centrifugation at 100 ***g*** for 8 min, and resuspended in 1 ml of RSB buffer containing 0.5% NP-40. The cells were homogenized by passing 10 times through a 23-gauge needle using a 1 ml syringe. The whole-cell fraction was harvested. After centrifugation at 100 ***g*** for 8 min, the NP-40 supernatant fraction was obtained from the supernatant. The pellet was then resuspended in 375 µl of sucrose buffer 1 (250 mM sucrose, and 10 mM $MgCl_2$), overlaid onto 500 µl of sucrose buffer 2 (880 mM sucrose and 50 mM $MgCl_2$), and then purified by centrifugation at 400 ***g*** for 10 min. The pelleted nuclei were resuspended in 200 µl of sucrose buffer 3 (340 mM sucrose and 50 mM $MgCl_2$) and sonicated for 60 s (10 s intervals). The sonicated cell lysate was then overlaid onto 200 µl of sucrose buffer 2 and centrifuged at 10,200 ***g*** for 20 min. The pellet and the supernatant were harvested and subjected to immunoblotting. All buffers contained multiple protease inhibitors.

Plasmids

pCLMSCVhyg-HA-GRWD1, pGEX-6P-2-GRWD1, pFLAG-CMV-5a-RPL5, pFLAG-CMV-5a-RPL11, pcDNA3.1-HA-Ub, pCLH'CX-HA-GRWD1, pAcGFP1-Mem, pcDNA4/Hismax-MDM2, pFLAG-CMV-5b-HA-GRWD1, and the GRWD1 truncated mutant expression vectors were described previously (Kayama et al., 2017; Sugimoto et al., 2008). pCMV-Tag2B-EDD was purchased from Addgene (#37188; Cambridge, MA). pFLAG-CMV-5a-RPL23 was generated by inserting RPL23 cDNA (from pCMV-SPORT6; OpenBiosystems, Boston, MA) into pFLAG-CMV-5a using the In-Fusion HD cloning system (Clontech, Mountain View, CA). The following primers were used: 5′-GAACCGTCAGAATT-CACCATGTCGAAGCGAGGACG-3′ (RPL23 forward) and 5′-ACCGGATCCGTCGACTGC-AATGCTGCCAGCATTGGA-3′ (RPL23 reverse). pGEX6P-1-RPL23 was constructed by inserting RPL23 cDNA into pGEX6P-1 (GE Healthcare, Boston, MA). pCLH'CX-His-T7-RPL23 was constructed as described below. RPL23 cDNA was inserted into pET-28a. Then, pENTR4-His-T7-RPL23 was generated by inserting the His-T7-RPL23 region from pET-28a-RPL23. Subsequently, the His-T7-RPL23 region from pENTR4-His-T7-RPL23 was inserted into pDEST-CLH'CX using the Gateway reaction (Invitrogen, Carlsbad, CA).

GRWD1 cDNA was inserted into pFLAG-CMV-5b (Sigma) using the In-Fusion HD cloning system (Clontech) to create pCMV-GRWD1 which expresses non-tagged GRWD1. The following primers were used: forward, 5′-TGGAAGCTTGCGGCCGCCACCATGGCCGCGCGCAAGGGA-3′; and reverse, 5′-GATAGATCTGCGGCCGCTCAGACAA-3′.

Journal of Cell Science (2018) 131, jcs213009. doi:10.1242/jcs.213009

GRWD1 cDNA was also inserted into pAAVS1 CMV-MCS-PURO (Natsume et al., 2016) using the In-Fusion HD cloning system (Clontech) to create pAAVS1 CMV-GRWD1-PURO. The following primers were used: forward, 5′-ACCGGACTCAGATCTGCCACCATGGCCGCGCGCAAG-GGA-3′; and reverse, 5′-CGCGGTACCGTCGACTCAGACACTGATG-GTGCGGAAG-3′.

Transfection

For Fig. 1B,C, 293T cells in 100 mm dishes (4×10^6 cells/dish) were transiently transfected with the indicated expression vectors (6 µg total) using TransIT-293 reagent (Mirus, Madison, WI) according to the manufacturer's instructions. At 48 h after transfection, cells were subjected to immunoprecipitation.

For Figs 2B and 3C, HCT116 cells in 100 mm dishes (6×10^6 cells/dish) were transiently transfected with the indicated expression vectors (12 µg) using PEImax (Polysciences, Warrington, PA), as described previously (Sugimoto et al., 2015). At 42 h after transfection, cells were subjected to immunoprecipitation or fractionation assay.

For Figs 3A, 5D and 7A, and Figs S2 and S4A, cells in 12-well plates (10^5 cells/well) were transiently transfected with the expression vectors (0.8 µg total) using PEImax. At 42 h (Fig. 3A; Fig. S2) or 48 h (Figs 5D, 7A; Fig. S4A) post transfection, cells were subjected to immunoblotting.

For Fig. 3B and 3E, HCT116 cells in 12-well plates (10^5 cells/well) were transiently transfected with expression vectors (0.8 µg total) using PEImax. At 30 h after transfection, cells were treated with 25 µM MG132 (PEPTIDE Institute, Osaka, Japan) or DMSO as a control for a further 12 h and then subjected to immunoblotting.

For Figs 5B,C and 6 and Fig. S4B, 293T cells in 100 mm dishes (3×10^6 cells/dish) were transiently transfected with the indicated expression vectors using PEImax (12 µg total; Fig. 5B,C and Fig. S4B) or TransIT-293 (3 µg total; Fig. 6). At 42 h (Fig. 5B) or 48 h (Figs 5C, 6 and Fig. S4B) after transfection, cells were subjected to immunoprecipitation, or a pulldown assay or *in vivo* ubiquitylation assay.

siRNA experiments

For Fig. 4A, left panel, B,C and Fig. S3, cells in 12-well plates (1×10^5 cells/well) were transfected with 18 pmol siRNA duplexes using Lipofectamine RNAiMAX (Invitrogen) according to the manufacturer's instructions. For Fig. 4A, right panel, cells in 6-well plates (1.5×10^5 cells/well) were transfected with 22 pmol siRNA duplexes as described above. siRNA oligonucleotides were synthesized (IDT, Coralville, IA) with the following sequences (sense strand): siRNA against EDD, siEDD-1, 5′-GGAGAGC-CAAACUUGGAUAAGAAdGdA-3′ and siEDD-2, 5′-GCACUUCAGU-UCUAACUAGACAUdTdT-3′. The sequences of siRNA against GRWD1 (siGRWD1-1, siGRWD1-3 and siGRWD1-4) and controls (DS scrambled Neg, siLuci, siGFP) were described previously (Kayama et al., 2017).

Immunoblotting and antibodies

Immunoblotting and quantification of band signals were performed as described previously (Sugimoto et al., 2008, 2015). Preparation of polyclonal rabbit antibodies against GRWD1 (1:400), CDC6 (1:200), MCM7 (1:2000), and RPL11 (1:50) was described previously (Fujita et al., 1996, 1999; Kayama et al., 2017; Sugimoto et al., 2008). The anti-human EDD antibody (1:1000) was obtained by immunizing rabbits with the human EDD peptide (KWSESEPYRNAQNPS). Other antibodies were purchased from the following companies: α-tubulin (ab15246, Abcam, Cambridge, UK; 1:200), Cul4a (A300-739A, Bethyl, Montgomery, TX; 1:1000), DDB1 (A300-462A, Bethyl; 1:1000), fibrillarin (ab4566, Abcam; 1:2000), FLAG (PA1-984B, Thermo Scientific, Waltham, MA; 1:500), GST (G7781, Sigma, 1:2000), GFP (A6455, Invitrogen; 1:1000), HA (MMS-101R, Covance, Princeton, NJ; 1:1000), MDM2 (OP46, Calbiochem, San Diego, CA; 1:100), p53 (OP43, Calbiochem; 1:1000), PCNA (M0879, DAKO, Santa Clara, CA; 1:100), RFC4 (sc-20996, Santa Cruz, Santa Cruz, CA; 1:100), RPL3 (GTX114725, GeneTex, Irvine, CA; 1:500), RPL5 (ab86863, Abcam; 1:500), RPL23 (ab156813, Abcam; 1:500), RuvBL2 (#8959, Cell Signaling Technology, Danvers, MA; 1:1000), SMC4 (61130, Active Motif, Carlsbad, CA; 1:750), T7 (69522-3, Millipore, Billerica, MA; 1:10,000) and ubiquitin (#3936, Cell Signaling Technology; 1:1000).

Quantification of chemiluminescent signals

Chemiluminescent signals were captured using a cooled CCD camera-directed detection system (LumiVision Imager, Aisin, Aichi, Japan) within the linear range, and band intensities were quantified using LumiVision Analyzer 130 (Aisin). Specific signals then calculated by subtracting background signal. The obtained signals were then normalized to the signal generated by control proteins [GFP or Coomassie Brilliant Blue (CBB)-stained bands]. Signals generated by CBB bands were captured by CanoScan LiDE210 (Canon, Tokyo, Japan), and band intensities were quantified using ImageJ software.

In vivo ubiquitylation assay

293T cells were transiently transfected with the indicated expression vectors and/or empty vectors in various combinations for 36 h. Cells were further treated with 25 µM MG132 for 12 h before harvest. Cells were then lysed on ice in 1 ml RIPA buffer (50 mM Tris-HCl pH 7.4, 150 mM NaCl, 1% Triton X-100, 0.1% SDS and 0.5% sodium deoxycholate) containing 1 mM DTT and multiple protease inhibitors, and the soluble fractions were separated by centrifugation (13,600 ***g*** for 15 min). Lysates were immunoprecipitated with anti-RPL23 antibody (2 µg) and protein G–Sepharose beads, and the beads were washed three times with 1 ml NET gel buffer. The immunoprecipitates were subjected to SDS-PAGE followed by immunoblotting. Samples were adjusted to equalize the level of immunoprecipitated RPL23.

GST pulldown assay

GST-RPL23 or GST was bacterially expressed and purified on glutathione beads as described previously (Sugimoto et al., 2004). For Fig. 2C, GST–RPL23 or GST was incubated with purified GRWD1–His (Aizawa et al., 2016) and then bound to glutathione beads. After washing four times with buffer A (20 mM Tris-HCl pH 7.4, 200 mM NaCl, 1 mM DTT, 0.1% Triton X-100 and 5% glycerol), the bound proteins were eluted and subjected to SDS-PAGE followed by immunoblotting.

For Fig. 5B, 293T cells were transiently transfected with the indicated expression vectors and lysed on ice in 1 ml NP-40 buffer containing 1 mM DTT and multiple protease inhibitors. The lysates were incubated with GST–RPL23 or GST bound to glutathione beads. After washing four times with 1 ml NET gel buffer, the bound proteins were eluted and subjected to SDS-PAGE followed by immunoblotting.

His pulldown assay

Recombinant RPL23, prepared from GST–RPL23 by digestion with PreScission Protease (GE Healthcare Life Sciences) was incubated with or without GRWD1–His (Aizawa et al., 2016) in buffer A and then bound to HIS-Select HC Nickel affinity Gel (Sigma). After washing four times with buffer B (50 mM sodium phosphate, 250 mM NaCl and 10 mM imidazole), bound proteins were eluted and subjected to SDS-PAGE followed by immunoblotting.

Reverse transcriptase-quantitative PCR assay

HeLa cells were transfected with control [mixture of siRNA against luciferase and GFP (siLuci and siGFP, respectively)] or GRWD1-targeting (mixture of siGRWD1-3 and -4) siRNAs for 48 h. Total RNA was purified by using the RNeasy Mini Kit (QIAGEN, Hilden, Germany) and reverse transcribed using the PrimeScript RT reagent kit (TaKaRa, Shiga, Japan) according to the manufacturer's instructions. *RPL23* mRNA levels were then quantified by quantitative PCR as described previously (Sugimoto et al., 2011). Primer sequences were as follows: RPL23 forward, 5′-TCC-AGCAGTGGTCATTCGACAA-3′ and reverse, 5′-TGCATACTGGTCC-TGTAATGGCA-3′; GAPDH forward, 5′-GCACCGTCAAGGCTGA-GAAAC-3′ and reverse, 5′-TGGTGAAGACGCCAGTGGA-3′.

The cycling parameters were set as follows: 1 min at 95°C and 50 cycles of 95°C for 30 s, 60°C for 30 s and 72°C for 30 s.

Establishment of HFF2/T cells stably expressing HA-GRWD1 and HCT116 cells stably expressing His-T7-RPL23

HFF2/T cells stably overexpressing HA–GRWD1 were established as previously described (Kayama et al., 2017). A HCT116 AAVS-GRWD1

clone overexpressing GRWD1 was established as described below. Parental cells were transfected with pAAVS1 CMV-GRWD1-PURO and AAVS1 T2 CRIPR in pX330 (Natsume et al., 2016) using Lipofectamine 2000 reagent (Invitrogen) according to the manufacturer's instructions, selected with puromycin (1 µg/ml) and cloned. HCT116 or HCT116 AAVS-GRWD1 cells were then infected with recombinant retrovirus encoding His–T7–RPL23 or the corresponding control retrovirus. Recombinant retroviruses were produced as described previously (Kayama et al., 2017). Infected cells were selected with hygromycin B (200 µg/ml) and subjected to a soft agar colony formation assay without cloning.

Soft agar colony formation assay

Cells were seeded in six-well plates (1.2×10^4 cells/well) in DMEM containing 20% FCS and 0.4% agarose with a 0.7% agarose underlay (SeaPlaque). Duplicate wells were prepared for each sample. The medium was replaced once per week. Colonies were analyzed after 3 weeks with a CKX41 microscope equipped with a DP21 digital camera (OLYMPUS, Tokyo, Japan). To count the colonies, photographs of 12 randomly selected microscope fields for each sample were acquired at a magnification of 100× and colonies over the indicated sizes were counted.

Data presentation and statistical analysis

Unless otherwise stated, quantitative data are represented as the mean±s.d. of three or more independent experiments. The number of experiments was chosen according to the standards of the field. No samples were excluded from analysis using pre-established criteria. For qualitative data and semi-quantitative data, a representative image from multiple independent experiments is shown; for all such figures, essentially the same results were obtained from multiple independent experiments. Statistical analyses were performed with a two-tailed Student's *t*-test using Microsoft Excel software or with one-way ANOVA and Tukey's multiple comparison test using R. $P<0.05$ was considered statistically significant.

Acknowledgements

We thank M. Kosugi and C. Sueyoshi for technical and secretarial assistance. We are also grateful for technical support from the Research Support Center, Graduate School of Medical Sciences, Kyushu University.

Competing interests

The authors declare no competing or financial interests.

Author contributions

Conceptualization: N.S., M.F.; Software: M.M., K.N.; Validation: S.W., M.M., K.N.; Formal analysis: S.W., H.F., T.T., K.K., M.M., K.N.; Investigation: S.W., H.F., T.T., K.K., M.M., K.N.; Data curation: S.W., M.M., K.N., N.S.; Writing - original draft: S.W.; Writing - review & editing: N.S., M.F.; Supervision: K.Y., M.F.; Project administration: N.S., M.F.; Funding acquisition: N.S., M.F.

Funding

This work was supported in part by grants from the Ministry of Education, Culture, Sports, Science and Technology of Japan to M.F. (21370084 and 25291027) and N.S. (25870509, 15K18412 and 18K07201) and by a grant to N.S. from the Uehara Memorial Foundation.

Supplementary information

Supplementary information available online at
http://jcs.biologists.org/lookup/doi/10.1242/jcs.213009.supplemental

References

Aizawa, M., Sugimoto, N., Watanabe, S., Yoshida, K. and Fujita, M. (2016). Nucleosome assembly and disassembly activity of GRWD1, a novel Cdt1-binding protein that promotes pre-replication complex formation. *Biochim. Biophys. Acta* **1863**, 2739-2748.

Bhat, K. P., Itahana, K., Jin, A. and Zhang, Y. (2004). Essential role of ribosomal protein L11 in mediating growth inhibition-induced p53 activation. *EMBO J.* **23**, 2402-2412.

Bursac, S., Brdovcak, M. C., Pfannkuchen, M., Orsolic, I., Golomb, L., Zhu, Y., Katz, C., Daftuar, L., Grabusic, K., Vukelic, I. et al. (2012). Mutual protection of ribosomal proteins L5 and L11 from degradation is essential for p53 activation upon ribosomal biogenesis stress. *Proc. Natl. Acad. Sci. USA* **109**, 20467-20472.

Clancy, J. L., Henderson, M. J., Russell, A. J., Anderson, D. W., Bova, R. J., Campbell, I. G., Choong, D. Y. H., Macdonald, G. A., Mann, G. J., Nolan, T. et al. (2003). EDD, the human orthologue of the hyperplastic discs tumour suppressor gene, is amplified and overexpressed in cancer. *Oncogene* **22**, 5070-5081.

Cmejla, R., Cmejlova, J., Handrkova, H., Petrak, J. and Pospisilova, D. (2007). Ribosomal protein S17 gene (RPS17) is mutated in diamond-blackfan anemia. *Hum. Mutat.* **28**, 1178-1182.

Dai, M.-S. and Lu, H. (2004). Inhibition of MDM2-mediated p53 ubiquitination and degradation by ribosomal protein L5. *J. Biol. Chem.* **279**, 44475-44482.

Dai, M.-S., Zeng, S. X., Jin, Y., Sun, X.-X., David, L. and Lu, H. (2004). Ribosomal protein L23 activates p53 by inhibiting MDM2 function in response to ribosomal perturbation but not to translation inhibition. *Mol. Cell. Biol.* **24**, 7654-7668.

Du, Y.-C. N. and Stillman, B. (2002). Yph1p, an ORC-interacting protein: potential links between cell proliferation control, DNA replication, and ribosome biogenesis. *Cell* **109**, 835-848.

Ellison, V. and Stillman, B. (2001). Opening of the clamp: an intimate view of an ATP-driven biological machine. *Cell* **106**, 655-660.

Fogeron, M.-L., Müller, H., Schade, S., Dreher, F., Lehmann, V., Kühnel, A., Scholz, A.-K., Kashofer, K., Zerck, A., Fauler, B. et al. (2013). LGALS3BP regulates centriole biogenesis and centrosome hypertrophy in cancer cells. *Nat. Commun.* **4**, 1531.

Fuja, T. J., Lin, F., Osann, K. E. and Bryant, P. J. (2004). Somatic mutations and altered expression of the candidate tumor suppressors CSNK1 epsilon, DLG1, and EDD/hHYD in mammary ductal carcinoma. *Cancer Res.* **64**, 942-951.

Fujita, M., Kiyono, T., Hayashi, Y. and Ishibashi, M. (1996). hCDC47, a human member of the MCM family dissociation of the nucleus-bound form during S phase. *J. Biol. Chem.* **271**, 4349-4354.

Fujita, M., Yamada, C., Goto, H., Yokoyama, N., Kuzushima, K., Inagaki, M. and Tsurumi, T. (1999). Cell cycle regulation of human CDC6 protein. intracellular localization, interaction with the human mcm complex, and CDC2 kinase-mediated hyperphosphorylation. *J. Biol. Chem.* **274**, 25927-25932.

Gamalinda, M., Ohmayer, U., Jakovljevic, J., Kumcuoglu, B., Woolford, J., Mbom, B., Lin, L. and Woolford, J. L. Jr (2014). A hierarchical model for assembly of eukaryotic 60S ribosomal subunit domains. *Genes Dev.* **28**, 198-210.

Gratenstein, K., Heggestad, A. D., Fortun, J., Notterpek, L., Pestov, D. G. and Fletcher, B. S. (2005). The WD-repeat protein GRWD1: potential roles in myeloid differentiation and ribosome biogenesis. *Genomics* **85**, 762-773.

Haga, K., Ohno, S., Yugawa, T., Narisawa-Saito, M., Fujita, M., Sakamoto, M., Galloway, D. A. and Kiyono, T. (2007). Efficient immortalization of primary human cells by p16INK4a-specific short hairpin RNA or bmi-1, combined with introduction of hTERT. *Cancer. Sci.* **98**, 147-154.

Harlow, E. and Lane, D. (1988). *Using antibodies: A Laboratory Manual*. New York: Cold Spring Harbor Laboratory Press.

He, Y. J., McCall, C. M., Hu, J., Zeng, Y. and Xiong, Y. (2006). DDB1 functions as a linker to recruit receptor WD40 proteins to CUL4-ROC1 ubiquitin ligases. *Genes Dev.* **20**, 2949-2954.

Higa, L. A., Wu, M., Ye, T., Kobayashi, R., Sun, H. and Zhang, H. (2006). CUL4-DDB1 ubiquitin ligase interacts with multiple WD40-repeat proteins and regulates histone methylation. *Nat. Cell Biol.* **8**, 1277-1283.

Honda, Y., Tojo, M., Matsuzaki, K., Anan, T., Matsumoto, M., Ando, M., Saya, H. and Nakao, M. (2002). Cooperation of HECT-domain ubiquitin ligase hHYD and DNA topoisomerase II-binding protein for DNA damage response. *J. Biol. Chem.* **277**, 3599-3605.

Iapalucci-Espinoza, S. and Franze-Fernández, M. T. (1979). Effect of protein synthesis inhibitors and low concentrations of actinomycin D on ribosomal RNA synthesis. *FEBS Lett.* **107**, 281-284.

Iouk, T. L., Aitchison, J. D., Maguire, S. and Wozniak, R. W. (2001). Rrb1p, a yeast nuclear WD-repeat protein involved in the regulation of ribosome biosynthesis. *Mol. Cell. Biol.* **21**, 1260-1271.

Jin, A., Itahana, K., O'Keefe, K. and Zhang, Y. (2004). Inhibition of HDM2 and activation of p53 by ribosomal protein L23. *Mol. Cell. Biol.* **24**, 7669-7680.

Jung, H.-Y., Wang, X., Jun, S. and Park, J.-I. (2013). Dyrk2-associated EDD-DDB1-VprBP E3 ligase inhibits telomerase by TERT degradation. *J. Biol. Chem.* **288**, 7252-7262.

Kayama, K., Watanabe, S., Takafuji, T., Tsuji, T., Hironaka, K., Matsumoto, M., Nakayama, K. I., Enari, M., Kohno, T., Shiraishi, K. et al. (2017). GRWD1 negatively regulates p53 via the RPL11-MDM2 pathway and promotes tumorigenesis. *EMBO Rep.* **18**, 123-137.

Killian, A., Le Meur, N., Sesboüé, R., Bourguignon, J., Bougeard, G., Gautherot, J., Bastard, C., Frébourg, T. and Flaman, J.-M. (2004). Inactivation of the RRB1-pescadillo pathway involved in ribosome biogenesis induces chromosomal instability. *Oncogene* **23**, 8597-8602.

Macias, E., Jin, A., Deisenroth, C., Bhat, K., Mao, H., Lindstrom, M. S. and Zhang, Y. (2010). An ARF-independent c-MYC-activated tumor suppression pathway mediated by ribosomal protein-Mdm2 interaction *Cancer. Cell* **18**, 231-243.

Maddika, S. and Chen, J. (2009). Protein kinase DYRK2 is a scaffold that facilitates assembly of an E3 ligase. *Nat. Cell Biol.* **11**, 409-419.

Meng, X., Tackmann, N. R., Liu, S., Yang, J., Dong, J., Wu, C., Cox, A. D. and Zhang, Y. (2016). RPL23 links oncogenic RAS signaling to p53-mediated tumor suppression. *Cancer Res.* **76**, 5030-5039.

Morgado-Palacin, L., Varetti, G., Llanos, S., Gómez-López, G., Martinez, D. and Serrano, M. (2015). Partial loss of Rpl11 in adult mice recapitulates diamond-blackfan anemia and promotes lymphomagenesis. *Cell Rep.* **13**, 712-722.

Natsume, T., Kiyomitsu, T., Saga, Y. and Kanemaki, M. T. (2016). Rapid protein depletion in human cells by auxin-inducible degron tagging with short homology donors. *Cell Rep.* **15**, 210-218.

Nicolas, E., Parisot, P., Pinto-Monteiro, C., de Walque, R., De Vleeschouwer, C. and Lafontaine, D. L. J. (2016). Involvement of human ribosomal proteins in nucleolar structure and p53-dependent nucleolar stress. *Nat. Commun.* **7**, 11390.

Nishimura, K., Kumazawa, T., Kuroda, T., Katagiri, N., Tsuchiya, M., Goto, N., Furumai, R., Murayama, A., Yanagisawa, J. and Kimura, K. (2015). Perturbation of ribosome biogenesis drives cells into senescence through 5S RNP-mediated p53 activation. *Cell Rep.* **10**, 1310-1323.

O'Donnell, M., Jeruzalmi, D. and Kuriyan, J. (2001). Clamp loader structure predicts the architecture of DNA polymerase III holoenzyme and RFC. *Curr. Biol.* **11**, R935-R946.

Pausch, P., Singh, U., Ahmed, Y. L., Pillet, B., Murat, G., Altegoer, F., Stier, G., Thoms, M., Hurt, E., Sinning, I. et al. (2015). Co-translational capturing of nascent ribosomal proteins by their dedicated chaperones. *Nat. Commun.* **6**, 7494.

Perry, R. P. and Kelley, D. E. (1970). Inhibition of RNA synthesis by actinomycin D: characteristic dose-response of different RNA species. *J. Cell. Physiol.* **76**, 127-139.

Pestov, D. G., Strezoska, Z. and Lau, L. F. (2001). Evidence of p53-dependent cross-talk between ribosome biogenesis and the cell cycle: effects of nucleolar protein Bop1 on G(1)/S transition. *Mol. Cell. Biol.* **21**, 4246-4255.

Rao, S., Lee, S.-Y., Gutierrez, A., Perrigoue, J., Thapa, R. J., Tu, Z., Jeffers, J. R., Rhodes, M., Anderson, S., Oravecz, T. et al. (2012). Inactivation of ribosomal protein L22 promotes transformation by induction of the stemness factor, Lin28B. *Blood* **120**, 3764-3773.

Rotin, D. and Kumar, S. (2009). Physiological functions of the HECT family of ubiquitin ligases. *Nat. Rev. Mol. Cell Biol.* **10**, 398-409.

Schaper, S., Fromont-Racine, M., Linder, P., de la Cruz, J., Namane, A. and Yaniv, M. (2001). A yeast homolog of chromatin assembly factor 1 is involved in early ribosome assembly. *Curr. Biol.* **11**, 1885-1890.

Subbaiah, V. K., Zhang, Y., Rajagopalan, D., Abdullah, L. N., Yeo-Teh, N. S. L., Tomaić, V., Banks, L., Myers, M. P., Chow, E. K. and Jha, S. (2016). E3 ligase EDD1/UBR5 is utilized by the HPV E6 oncogene to destabilize tumor suppressor TIP60. *Oncogene* **35**, 2062-2074.

Sugimoto, N., Tatsumi, Y., Tsurumi, T., Matsukage, A., Kiyono, T., Nishitani, H. and Fujita, M. (2004). Cdt1 phosphorylation by cyclin A-dependent kinases negatively regulates its function without affecting geminin binding. *J. Biol. Chem.* **279**, 19691-19697.

Sugimoto, N., Kitabayashi, I., Osano, S., Tatsumi, Y., Yugawa, T., Narisawa-Saito, M., Matsukage, A., Kiyono, T. and Fujita, M. (2008). Identification of novel human Cdt1-binding proteins by a proteomics approach: Proteolytic regulation by APC/CCdh1. *Mol. Biol. Cell* **19**, 1007-1021.

Sugimoto, N., Yugawa, T., Iizuka, M., Kiyono, T. and Fujita, M. (2011). Chromatin remodeler sucrose nonfermenting 2 homolog (SNF2H) is recruited onto DNA replication origins through interaction with Cdc10 protein-dependent transcript 1 (Cdt1) and promotes pre-replication complex formation. *J. Biol. Chem.* **286**, 39200-39210.

Sugimoto, N., Maehara, K., Yoshida, K., Yasukouchi, S., Osano, S., Watanabe, S., Aizawa, M., Yugawa, T., Kiyono, T., Kurumizaka, H. et al. (2015). Cdt1-binding protein GRWD1 is a novel histone-binding protein that facilitates MCM loading through its influence on chromatin architecture. *Nucleic Acids Res.* **43**, 5898-5911.

Takafuji, T., Kayama, K., Sugimoto, N. and Fujita, M. (2017). GRWD1, a new player among oncogenesis-related ribosomal/nucleolar proteins. *Cell. Cycle* **16**, 1397-1403.

Tatsumi, Y., Sugimoto, N., Yugawa, T., Narisawa-Saito, M., Kiyono, T. and Fujita, M. (2006). Deregulation of Cdt1 induces chromosomal damage without rereplication and leads to chromosomal instability. *J. Cell. Sci.* **119**, 3128-3140.

Trzcińska, A. M., Girstun, A., Piekiełko, A., Kowalska-Loth, B. and Staroń, K. (2002). Potential protein partners for the N-terminal domain of human topoisomerase I revealed by phage display. *Mol. Biol. Rep.* **29**, 347-352.

Tsurimoto, T. and Stillman, B. (1989). Purification of a cellular replication factor, RF-C, that is required for coordinated synthesis of leading and lagging strands during simian virus 40 DNA replication in vitro. *Mol. Cell. Biol.* **9**, 609-619.

Tsurimoto, T. and Stillman, B. (1990). Functions of replication factor C and proliferating-cell nuclear antigen: functional similarity of DNA polymerase accessory proteins from human cells and bacteriophage T4. *Proc. Natl. Acad. Sci. USA* **87**, 1023-1027.

Wan, C., Borgeson, B., Phanse, S., Tu, F., Drew, K., Clark, G., Xiong, X., Kagan, O., Kwan, J., Bezginov, A. et al. (2015). Panorama of ancient metazoan macromolecular complexes. *Nature* **525**, 339-344.

Wang, X., Singh, S., Jung, H.-Y., Yang, G., Jun, S., Sastry, K. J. and Park, J.-I. (2013). HIV-1 vpr protein inhibits telomerase activity via the EDD-DDB1-VPRBP E3 ligase complex. *J. Biol. Chem.* **288**, 15474-15480.

Zhang, Y., Shi, Y., Li, X., Du, W., Luo, G., Gou, Y., Wang, X., Guo, X., Liu, J., Ding, J. et al. (2010). Inhibition of the p53-MDM2 interaction by adenovirus delivery of ribosomal protein L23 stabilizes p53 and induces cell cycle arrest and apoptosis in gastric cancer. *J. Gene Med.* **12**, 147-156.

Zhang, Y.-F., Zhang, B.-C., Zhang, A.-R., Wu, T.-T., Liu, J., Yu, L.-F., Wang, W.-X., Gao, J.-F., Fang, D.-C. and Rao, Z.-G. (2013). Co-transduction of ribosomal protein L23 enhances the therapeutic efficacy of adenoviral-mediated p53 gene transfer in human gastric cancer. *Oncol. Rep.* **30**, 1989-1995.